# Updated Results of Singlet Oxygen Modeling Incorporating Local Vascular Diffusion for PDT

Rozhin Penjweini [1] and Timothy C. Zhu [1, *]
[1] Department of Radiation Oncology, University of Pennsylvania, Philadelphia, PA
* Corresponding author: tzhu@mail.med.upenn.edu

**Abstract:** Singlet oxygen ($^1O_2$) has a critical role in the cell-killing mechanism of photodynamic therapy. In this study, the distance-dependent $^1O_2$ is numerically calculated using finite-element method. Herein, we use a model that incorporates the diffusion equation for the light transport in tissue and the macroscopic kinetic equations for the $^1O_2$ generation. In addition, the model includes the microscopic kinetic equations of oxygen diffusion from uniformly distributed blood vessels to the adjacent tissue. The blood vessel network is assumed to form uniformly distributed Krogh cylinders and the spacing between vascular cylinders is varying between 18 and 60 μm. The cylindrical blood capillary has radius and mean length in the ranges of 2.5-10 μm and 100-400μm, respectively. For tumor vasculature, the oxygen pressure at aortal entrance of the blood vessel is assumed to be 50mmHg. The blood velocity in capillary is also considered to be in a range of 50-200μm/s.

**Keywords:** Photodynamic therapy, singlet oxygen generation, initial oxygen concentration, oxygen supply rate, macroscopic model.

## 1. Introduction

Photodynamic therapy (PDT) has received much attention in recent years due to its use to treat proliferative disorders, including cancer [1]. Conventional PDT involves the administration of a photosensitizer drug (PS), which preferentially accumulates in diseased cells, followed by a continuous excitation of specific wavelengths [2,3]. Most PSs generate fluorescence and reactive oxygen species upon light irradiation [2,4]. In type-II PDT, singlet oxygen ($^1O_2$) is the major cytotoxic agent causing biological and therapeutic effects [4,5]. In this study, the mathematical descriptions of the PDT photo-chemophysical reactions are used to calculate the spatiotemporal distributions of the Photofrin-mediated PDT components such as PS, $^1O_2$, ground triplet-state of oxygen $^3O_2$ as well as the maximum oxygen supply rate g. Figure 1 is the schematic images of PDT and our model.

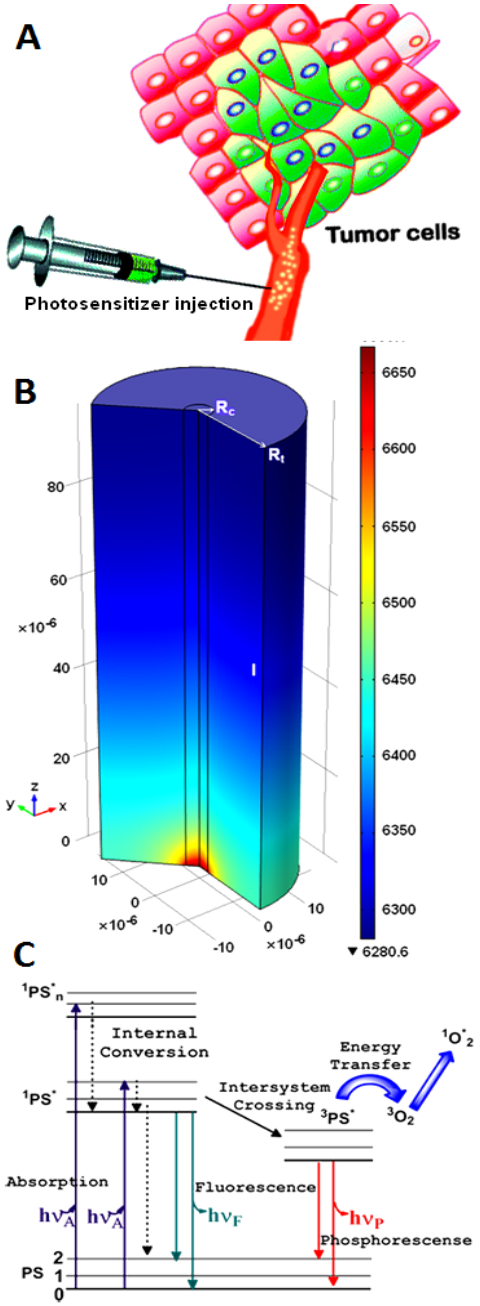


**Figure 1:** Schematic images of A) photosensitizer administration in PDT, B) Krogh cylinders model of the blood vessel network, C) Jablonski diagram [6] of the PDT photochemical reactions and mechanisms.

## 2. Theory

In our macroscopic model [4-8], the spatial distribution of light fluence rate $\phi$, temporal and spatial distribution of PS [$S_0$], [$^3O_2$] and [$^1O_2$] concentrations in tumor are obtained by:

$$\frac{d[S_0]}{dt} + \left( \xi\sigma \frac{\phi([S_0]+\delta)[^3O_2]}{[^3O_2]+\beta} \right)[S_0] = 0 \quad (1)$$

$$\frac{d[^3O_2]}{dt} + \left( \xi \frac{\phi[S_0](1+\sigma([S_0+\delta]))}{[^3O_2]+\beta} \right)[^3O_2] = \Gamma_s \quad (2)$$

$$\frac{d[^1O_2]_{rx}}{dt} - f.\left( \xi \frac{\phi[S_0][^3O_2]))}{[^3O_2]+\beta} \right) = 0 \quad (3)$$

where $\xi$, $\sigma$ and $\beta$ represent initial oxygen consumption rate, ratio of photobleaching to reaction between $^1O_2$ and biological targets, and ratio of triplet state phosphorescence to reaction between triplet excited state sensitizer T and $^3O_2$, respectively; $\delta$ is a constant.
In equation (2), the symbol $\Gamma_s$ denotes the rates at which ground-state oxygen is supplied to the surrounding tissue by:

$$\Gamma_s = g\left(1 - \frac{[^3O_2]}{[^3O_2](t=0)}\right) \quad (4)$$

where g represents a maximum supply rate and $[^3O_2]_0$ is the initial oxygen concentration at $t$= 0.
The concentration of oxygen is expressed using the partial pressure of oxygen (P):

$$[^3O_2] = \alpha P \quad (5)$$

The governing equations for the transport of oxygen and oxy-hemoglobin during PDT in our model is given by [4,7]:

$$C_H \frac{\partial S}{\partial t} = C_H D_H \nabla^2 S - \bar{v}.C_H \nabla S - \Gamma_{rec} \quad (6)$$

$$\alpha_c \frac{\partial P}{\partial t} = \alpha_c D_c \nabla^2 P - \bar{v}.\alpha_c \nabla P + \Gamma_{rec} \quad (7)$$

where S is hemoglobin oxygen saturation that describes the percentage of oxy-hemoglobin. $C_H$ is total hemoglobin concentration in capillary. The product of S and $C_H$ is oxy-hemoglobin concentration. In equations (6) and (7), the first term in the right side considers the hemoglobin and oxygen diffusion; the convection process is described by the second term. Herein, $\Gamma_{rec}$ represents the oxygen loading/unloading from deoxy-hemoglobin/oxy-hemoglobin.
The oxygen dissociation can be solved by the Hill's equation.

$$S = \frac{P^n}{P^n + P_{50}^n} \quad (8)$$

By manipulating the equations (6)-(8):

$$(\alpha_c + KC_H)\frac{\partial P}{\partial t} = (\alpha_c D_c + KC_H D_H)\nabla^2 P - (\nu_z \alpha_c + \nu_z KC_H)\frac{\partial P}{\partial z} + C_H D_H M\left(\left(\frac{\partial P}{\partial r}\right)^2 + \left(\frac{\partial P}{\partial z}\right)^2\right) \quad (9)$$

$$K = \frac{nP^{n-1}P_{50}^n}{(P^n + P_{50}^n)^2} \quad (10)$$

$$M = \frac{n(n-1)P_{50}^n P^{n-2}(P^n + P_{50}^n) - 2n^2 P^{(2n-2)} P_{50}^n}{(P^n + P_{50}^n)^3} \quad (11)$$

For the boundary conditions, the bottom end of capillary (i.e. z = 0) was considered to be the entrance of blood flow. On the boundary between capillary and tissue, both oxygen flux and partial pressure are assumed to be continuous. Therefore,

$$P\big|_{z=0,\, r\in[0,R_c]} = P_{ts} \quad (12)$$

$$D_c\alpha_c \nabla P\big|_{r=R_c^-} = D_t\alpha_t \nabla P\big|_{r=R_c^+} \quad (13)$$

$$P\big|_{r=R_c^-} = P\big|_{r=R_c^+} \quad (14)$$

$$\nabla P\big|_{other} = 0 \quad (15)$$

For oxygen in tissue:

$$\frac{\partial[^3O_2]}{\partial t} + \left(\xi \frac{\phi[S_0][^3O_2](1+\sigma([S_0]+\delta))}{[^3O_2]+\beta}\right) = D_t\nabla^2[^3O_2] - q_0 \frac{[^3O_2]}{[^3O_2]+\alpha_t P_m} \quad (16)$$

where, the first term of the right side considers the oxygen diffusion and the second term contains metabolic consumption.
Equations (16) has the same terms on the left-hand side as equation (2). More details of the equations can be found in references [4,5].

## 3. Use of COMSOL Multiphysics

The blood vessel network was assumed to form uniformly distributed Krogh cylinders. The forward calculation for $^1O_2$ generation model incorporating the macroscopic kinetic equations was done using COMSOL. Within COMSOL, the finite-element calculation was implemented by varying the input parameters of $\phi$, the spacing between vascular cylinders ($R_t$), blood capillary radius ($R_c$) and mean length ($l_z$) as well as the blood velocity in capillary ($v_z$). $[^3O_2]_0$ is considered to be less than 60 µM for tumor vasculature containing unstable endothelium and leaky vessels. This is achieved by setting the oxygen pressure ($P_{ts}$) at aortal entrance of the blood vessel to be 50 mmHg, lower than what was used for normal tissue at 80 mmHg. The initial Photofrin concentration in the tissue is assumed to be 7 µM and the total PDT time was chosen to be 100 minutes. PDT and vascular parameters used in the whole calculations are listed in tables 1 and 2, respectively.

**Table 1:** PDT photochemical parameters

| Parameters | Value |
|---|---|
| $\xi$ | $3.70\times10^3$ cm$^2$ mW$^{-1}$ s$^{-1}$ |
| $\sigma$ | $2.97\times10^{-5}$ µM$^{-1}$ |
| $\delta$ | 33 µM |
| $\beta$ | 8.7 µM |

In the first step, the differential equations were solved to account for the actual oxygen diffusion through the local vasculature. Then, volume-averaged quantities over the tissue cylinder $R_t$ was calculated for $[^3O_2]$, $[^1O_2]$ as well as the volume average over the whole tissue cylinder for left-hand side of equation (2) as the oxygen supply rate.
The more detailed description of the model and the fitting routine can be found in references [4,7].

## 4. Results and discussion

The distributions of the Photofrin-mediated PDT components such as PS, singlet oxygen $^1O_2$ and ground triplet-state of oxygen $^3O_2$ as well as the oxygen supply rate were averaged over the whole Krogh cylinder (see figure 2).

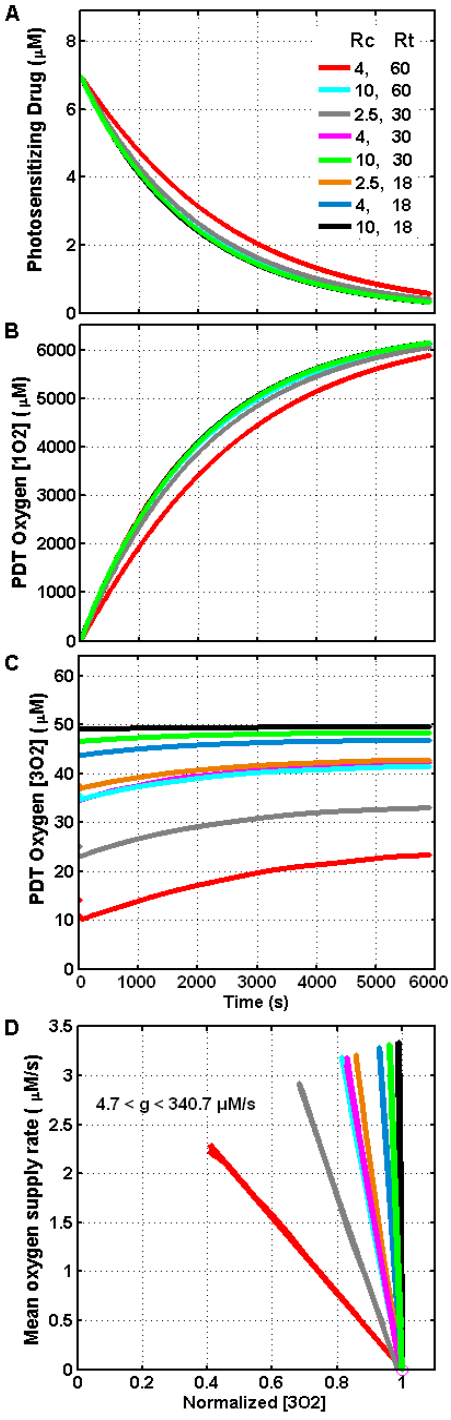


**Figure 2:** Changes of volume-averaged A) Photofrin PS, B) $^1O_2$, C) $^3O_2$ vs. time (100 min PDT). D) volume-averaged oxygen supply rate vs. normalized $^3O_2$ ($[^3O_2]/[^3O_2]_0$). Each plot contains 8 combinations of $R_c$= 2.5, 4, 10 µm and $R_t$= 18, 30, 60 µm. In all combinations, $l_z$ = 220 µm, $v_z$ = 100 µm/s, $q_0$= 2.4 µM/s, $P_{ts}$ = 50 mmHg and $\phi$ = 150 mW/cm$^2$.

**Table 2:** PDT parameters used for all calculations

| Parameters | Value |
|---|---|
| $R_c$ Capillary radius | 2.5-10 μm |
| $R_t$ Tissue radius | 18-60 μm |
| $D_t$ Oxygen tissue diffusion coefficient | 1700 $\mu m^2/s$ |
| $D_c$ Oxygen capillary diffusion coefficient | 1240$\mu m^2/s$ |
| $\alpha_t$ $^3O_2$ solubility in tissue | 1.30 μM/mmHg |
| $\alpha_c$ $^3O_2$ solubility in plasma | 1.53 μM/mmHg |
| $P_{ts}$ Artery $^3O_2$ partial pressure | 50 mmHg |
| $P_{50}$ Half-max hemoglobin saturation | 26 mmHg |
| $P_m$ Half-max oxygen consumption supply $pO_2$ | 0.39 mmHg |
| $C_H$ Plasma oxygen carrying capacity | 2500 μM |
| n Hill constant | 2.46 |
| $l_z$ Length of capillary | 100-400 μm |
| $v_z$ Blood flow velocity | 50-200 μm/s |
| $q_0$ Max $^3O_2$ metabolic consumption rate | 0.9-6 μM/s |

Different combinations of $R_c$= 2.5, 4, 10 μm and $R_t$= 18, 30, 60 μm were used to plot figure 2. As shown in figure 2-A, the average PS concentration is decreasing vs. time due to the photobleaching effect. All cases showed very similar amounts of photobleaching. However, photobleaching was minimum for $R_c$= 4 μm and $R_t$= 60 μm. The results presented in figure 2-B show that the average $^1O_2$ increases dramatically vs. time. After 100 min PDT, the obtained $^1O_2$ concentrations were about 6000 μM for all cases. A gradual increase was also obtained for the average concentration of $^3O_2$ (see figure 2-C). This increase is due to the photobleaching effect, which was estimated to be maximum for the combinations of $R_c$= 4 μm, $R_t$= 60 μm and $R_c$= 2.5 μm, $R_t$= 30 μm. To examine possible values of g, the volume-averaged oxygen supply rate was calculated as a function of normalized volume-averaged $^3O_2$ concentration ($[^3O_2]/[^3O_2]_0$). As shown in figure 2-D, in all combinations of $R_c$ and $R_t$, there is a linear relationship between the oxygen supply rate and normalized oxygen. However, g varies with the tissue radius and capillary radius; the obtained g values were in the range of 4.7-340.7 μM/s.

In the next step, the effects of capillary length $l_z$, blood flow velocity $v_z$, metabolism consumption of tissue $q_0$ as well as fluence rate $\phi$ on g values were investigated. The results are summarized in figure 3.

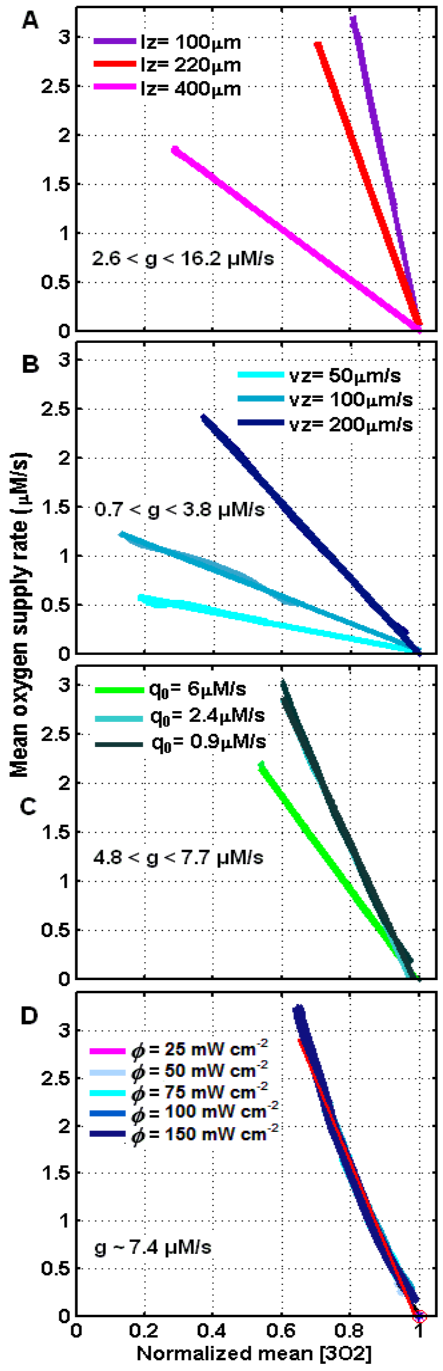


**Figure 3:** Calculated oxygen supply rate vs. $[^3O_2]/[^3O_2]_0$ for A) $R_c$= 2.5 μm, $R_t$= 30 μm, $q_0$= 2.4 μM/s, $v_z$ = 100 μm and $\phi$ = 150 mW/cm$^2$, B) $R_c$= 2.5 μm, $R_t$= 60 μm, $q_0$= 0.9 μM/s, $l_z$ = 220 μm, and $\phi$ = 150 mW/cm$^2$, C) $R_c$= 4 μm, $R_t$= 60 μm, $l_z$ = 220 μm, $v_z$ = 200 μm/s and $\phi$ = 150 mW/cm$^2$, D) $R_c$= 2.5 μm, $R_t$= 30 μm, $q_0$= 2.4 μM/s, $l_z$ = 220 μm and $v_z$ = 100 μm/s. In all cases $P_{ts}$ = 50 mmHg.

As shown in figures 3-A and B, g varies with the capillary length $l_z$ and the blood flow velocity $v_z$. In a capillary with $R_c$ = 2.5 and Rt = 30 μm, when the mean length $l_z$ increased from 100 μm to 400 μm, the resulting blood perfusion rate g decreases from 16.2 μM/s to 2.6 μM/s following roughly $1/l_z$. At the same conditions of $R_c$ = 2.5 and $R_t$ = 60 μm, when the blood velocity increased from 50 μm/s to 750 μm/s, g increased from 0.7 to 3.8 μM/s (see figure 3-B). The influence of the metabolism consumption of tissue $q_0$ is presented in figure 3-C. When $q_0$ decreased from 6 to 0.9 μM/s, g increased from 4.8 to 7.7 μM/s for otherwise the same conditions of $R_c$ = 4 and $R_t$ = 60 μm. However, $q_0$= 0.9 μM/s and 2.4 μM/s, showed very similar g values in the same capillary and tissue. Figure 3-D presents the effect of fluence rate $\phi$ on obtained g values. Based on figure 3-D, the linear relation between the oxygen supply rate and normalized oxygen is independent of the fluence rate. In all experimental fluence rates (25-150 mW/cm$^2$), the obtained g value was around 7.4 μM/s for the case of $R_c$ = 2.5 and $R_t$ = 30 μm.

## 5. Conclusions

The improvement of the model formulations have been made to prove the validity of the formulation of the oxygen perfusion term, $g(1-[^3O_2]/[^3O_2]_0)$, used in the macroscopic singlet oxygen model. The model was then investigated in a broad range of physiological parameters to examine possible values of g. In all cases the results show a linear relationship between the oxygen supply rate and normalized oxygen, which justifies the hypothesis of a linear expression for oxygen supply in the previous macroscopic model [4]. The variation of g was between 0.85-606.96 μM/s among the feasible parameters obtained from literature.

## 6. References


1. A. Juarranz, P. Jaén, F. Sanz-Rodríguez, J. Cuevas, S. González, Photodynamic therapy of cancer. Basic principles and applications, *Clin Transl Oncol*, **10**, 48-54 (2008)

2. R. Penjweini, H G. Loew, M. Eisenbauer, K W. Kratky, Modifying excitation light dose of novel photosensitizer PVP-Hypericin for photodynamic dynamic diagnosis and therapy, *J. Photochem. Photobiol. B, Biol*, **120**, 120-129 (2013)

3. R. Penjweini, H G. Loew, P. Breit, K W. Kratky, Optimizing the antitumor selectivity of PVP-Hypericin re A549 cancer cells and HLF normal cells through pulsed blue light, *Photodiagnosis and Photodynamic Therapy*, **10**, 591-599 (2013)

4. T C. Zhu, B. Liu, Singlet oxygen modeling of PDT incorporating local vascular oxygen diffusion, *Proceeding for the 2013 COMSOL conference in Boston.*

5. K. K-H Wang, J. C. Finlay, T. M. Busch, S. M. Hahn, T. C. Zhu, Explicit dosimetry for photodynamic therapy: macroscopic singlet oxygen modeling, *J. Biophotonics*, **3**, 304-318 (2010)

6. M. Ethirajan, Y. Chen, P. Joshi, R K. Pandey, The role of porphyrin chemistry in tumor imaging and photodynamic therapy. *Chem. Soc. Rev.*, **40**, 340-362 (2011)

7. K. K-H Wang, S. Mitra, T. H. Foster, A comprehensive mathematical model of microscopic dose deposition in photodynamic therapy, *Med. Phys*. **34**, 282-293 (2007)

8. T C. Zhu, J C. Finaly, X. Zhou, J. Li, Macroscopic modeling of the singlet oxygen production during PDT, *Proceeding SPIE, 6427, 642708* (2007).


## 7. Acknowledgements


We thank the useful discussion with Dr. Jarod C. Finlay on the theory. This work is supported by National Institute of Health (NIH) P01 CA87971 and R01 CA 154562 grants.